G.M. Katyba,[1,2,3,*] M. Skorobogatiy[3], N.V. Chernomyrdin[2,4], A.N. Perov[4], I.N. Dolganova[4]
D.G. Melikyants,[4] K.I. Zaytsev,[2,4] and V.N. Kurlov[1]

SAPPHIRE SHAPED CRYSTALS: FROM THZ-WAVE DELIVERY TO SUPER-RESOLUTION IMAGING

[1]Institute of Solid State Physics of RAS, Russia

[2]Prokhorov General Physics Institute of RAS, Russia

3 Department of Engineering Physics, Polytechnique Montreal, Canada

[4]Bauman Moscow State Technical University, Russia

*E-mail: katyba_gm@issp.ac.ru

Saratov Fall Meeting 2022, Advanced Materials for Optics & Biophotonics V, Saratov, Russia, 2022

OUTLINE OF THE TALK

- Optical elements designing for THz radiation delivery
  - Sapphire hollow-core waveguides for low-loss radiation delivery
- Attempts to improve the spatial resolution of THz imaging
  - Bundles of metal-coated sapphire fibers for THz sub-wavelength imaging
  - Tapered all-dielectric optical bundles for sub-wavelength imaging with using diffraction limited optics

Optical elements designing for THz radiation delivery

THz radiation

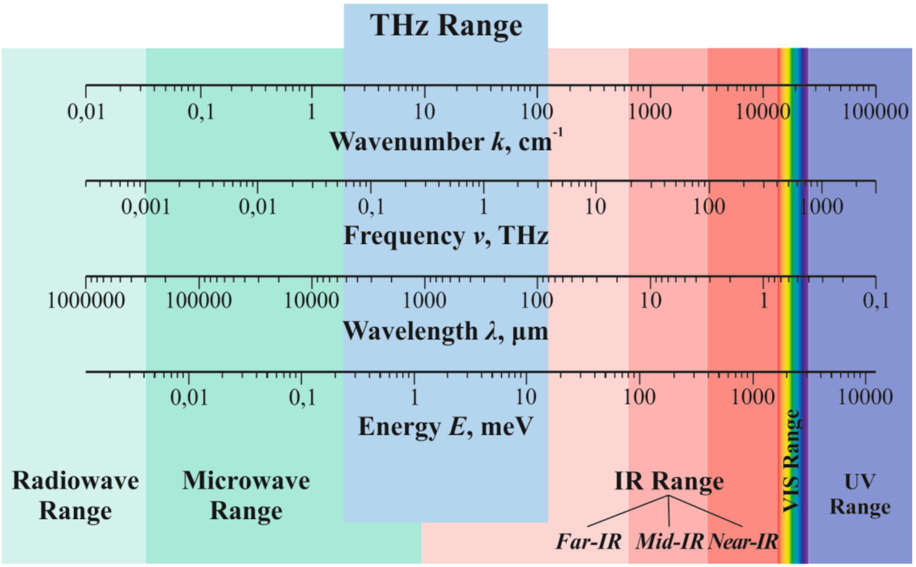

[H. Rubens & E. Nichols, "Heat rays of great wave length,"*Physical Review (Series I)* **4**, 314 (1897)]

Electromagnetic Radiation – Matter Interactions

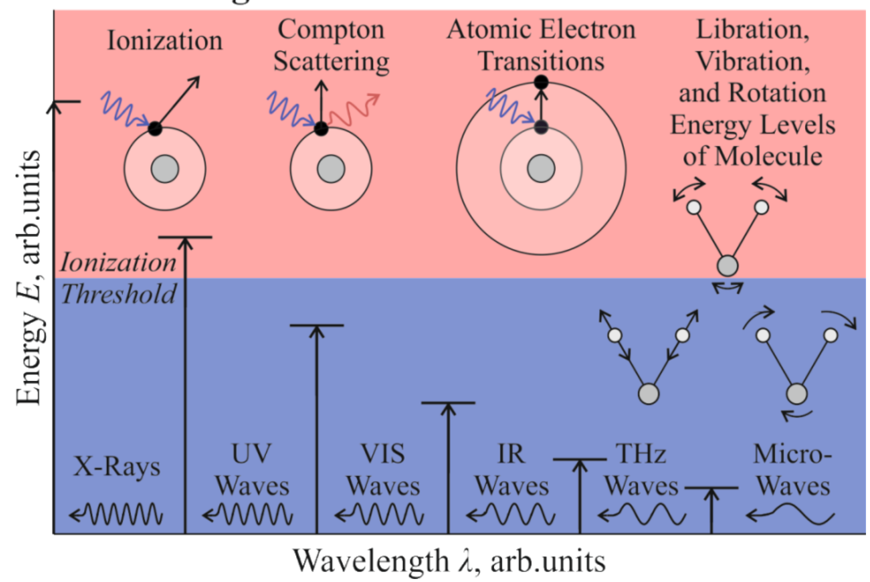

THz Pulsed Spectroscopy for Non-Destructive Evaluation of Polymers

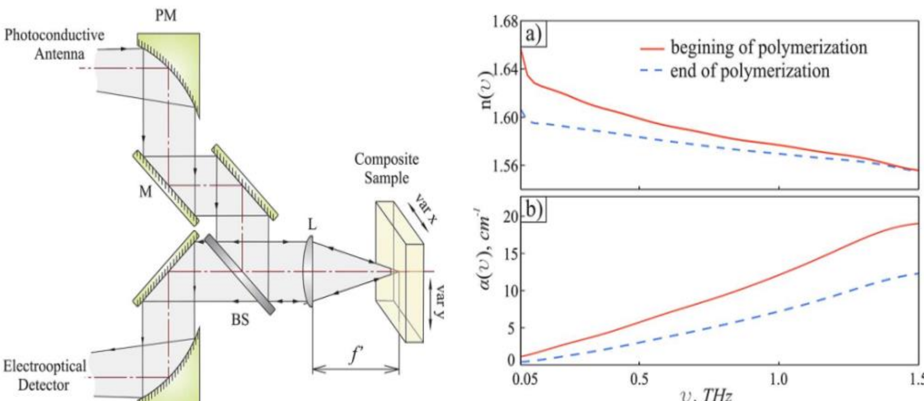

[K.I. Zaytsev et al, IEEE Tr.Ter.Tech., ***5****(5)*, 810 *(2015)]*

Broadband dielectric response of water

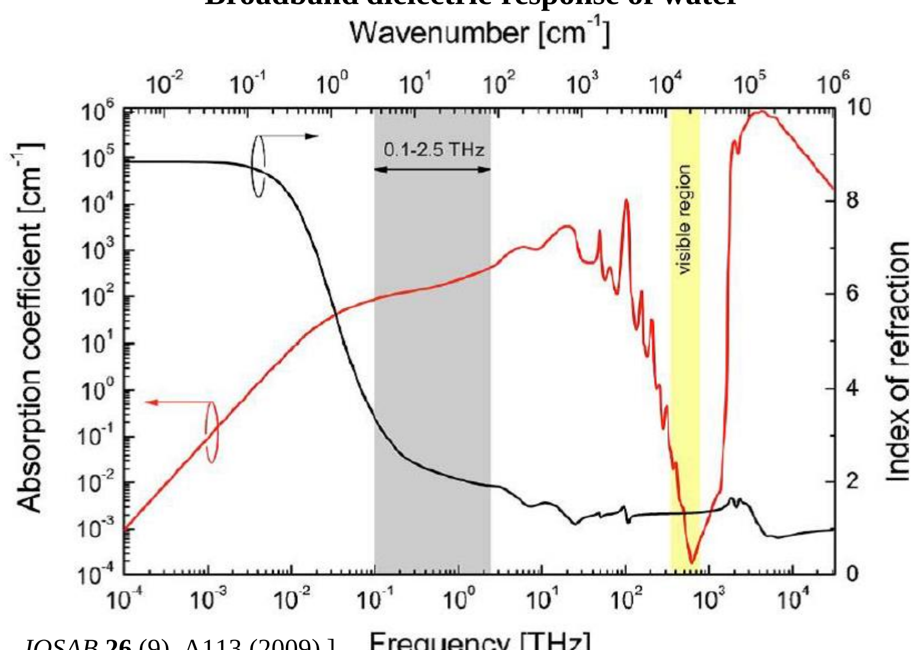

[U. Moller et al., *JOSAB* **26** (9), A113 (2009)]

THz Waveguiding Technologies

#	Waveguide	Cross-section	Spectral range, THz	Losses α, cm^{-1}	Material	Sizes	Comments
1	Parallel plate	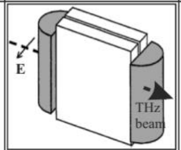	0.1 - 4.0	$\alpha < 0.1$ near $\nu = 0.4$, 1.4 and 2.8 THz; $\alpha > 0.2$ near 4.0 THz	Copper	Separation plate d=108 µm L=24.4 mm	Guiding mechanism: reflection from metal
2	Graded step-index	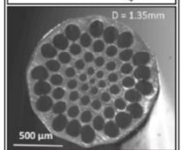	0.2 - 1.5	increase from 0.025 to 0.15	Low density polyethylene (LDPE); α_{mat}=0.2 cm^{-1}, for ν =1.0 THz	5 rings of holes D_{out}=1.35 mm L=20 cm	Guiding mechanism: total internal reflection (TIR); dispersion < 1 ps/THz/cm; single mode below 0.35 THz
3	Porous Step-index		0.2 - 0.4	$0.035+3.1\nu^2$ [THz^2]	Silk foam; n_{mat}=1.057 α_{mat}=0.9 for ν =0.3 THz	D_{out}=5 mm L=20 cm	Guiding mechanism: TIR; dispersion ≈ 10 ps/THz/cm; 94% porosity of material
4	Hollow tube	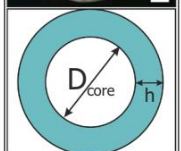	0.3 - 1.0	decrease from 0.05 to 0.5	Polymethyl-methacrylate (PMMA); α_{mat} = 21.0 cm^{-1}, for ν =1.0 THz	D_{core}= 4 mm h = 2.95 mm	Guiding mechanism: anti-resonant (ARROW); dispersion < 10 ps/THz/cm; high absorbing cladding
5	Hollow tube with coating		2.5	0.0011 cm^{-1}	Hollow tube: silica glass, Cladding: polystyrene+Ag	D_{core}= 2.2 mm L_{film}= 8.2 µm (Ag-film=1 µm)	Guiding mechanism: reflection/ARROW; CDP is used for PS-Ag deposit film
6	Two-wire plasmonic		0.03 - 0.5	increase from ~ 0.003 to 0.015	Wires: stainless steel, Cladding: Styrofoam	D_{wire}= 0.3 mm L= 24 cm wire separation: 0.5 cm	Guiding mechanism: plasmonic; demonstrated THz guiding through commercial TV-cable
7	Revolver multichannel	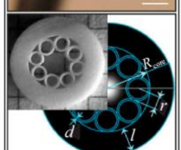	0.5 - 2.5	α_{min} = 0.017 ν = 2.1 THz	Polypropylene (PP) α_{mat} = 0.2 cm^{-1}, for ν =1.0 THz	d=0.06 mm r=0.4 mm D_{core}=1.3 mm D_{outer}=4.45 mm l=0.79 mm	Guiding mechanism: ARROW; dispersion< 1 ps/THz/cm; 3 transparency band near 0.7, 1.4, and 2.1 THz
8	PC omniguide	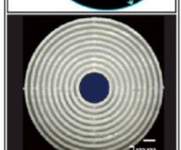	0.1 - 0.3	α_{min}=0.12 ν = 0.18 THz	Printing resin (PlasClear, Asiga) α_{mat} ≈ 1 cm^{-1}, for ν =0.18 THz	D_{core}=4.5 mm resin layer - 512 µm air layer - 512 µm $N_{bilayer}$=10	Guiding mechanism: Photonic Bandgap (PBG); have been used as a biosensor with sensitivity ≈ 0.1 GHz/µm

[G. Katyba et al., *Progress in Crystal Growth and Characterization of Materials* **67** (2021) 100523]

Mean features of **polymer** materials in THz:

- relatively low radiation losses;
- high manufacturability (it is possible to produce the waveguides with complex cross—sections);
- relatively low refractive index;
- high sensitivity to the outer environment (for the most polymers);
- high dispersion in many cases.

Mean features of **crystalline** materials in THz:

- low radiation losses and high refractive index;
- High resistivity (thermal, chemical, etc.)
- High hardness of material prevent to produce waveguides with complex shape

Moreover, all this types of THz waveguides can not be used for THz measurements in aggressive environments, in high temperature/pressure, in particular!

For example, they can damaged from medical sterilization

Shaped Sapphire – Key to THz delivery via hollow-core waveguides

Refractive index (a, c) and extinction coefficient (b, d) of sapphire

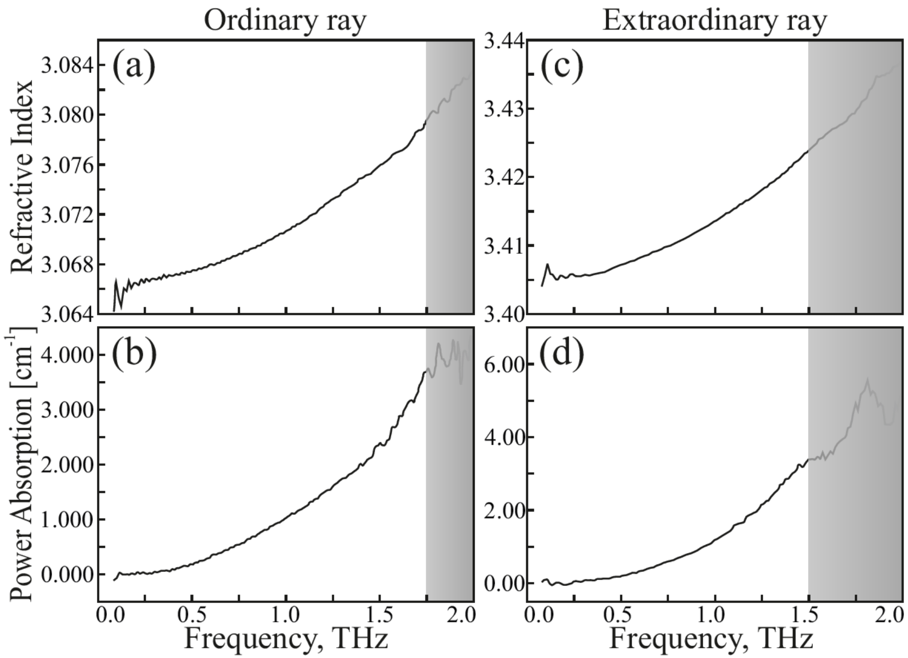

Transparancy and radiation strength	
Electromagnetic transparancy (or translucency)	0.2 μm < λ < 5 μm λ > 200 μm
Electromagnetic wave strength	Sustain high-power beams in VIS & IR spectral ranges
Radiation strength	No changes in IR transmission and VIS coloration after exposure to 10^7 - 10^8 Rad for 60 min at -195 °C

Thermal properties	
Melting point	2053 °C
Maximum use temperature	1800 °C
Thermal conductivity	41.9 W/(m·K)
hermal coefficient of expansion	5×10^{-6} - 5×10^{-6} K^{-1} at 323 K

- High melting point (higher then 2000 K)
- Broad transmission band spanning the UV, visible, and IR bands
- High tensile strength
- High chemical and thermal shock resistance
- Biocompatibility
- High hardness (9 degree on Mohs scale)
- High specific heat
- Low friction coefficient ((3.24-5.66)10^6 K^{-1})

Shaped crystal growth techniques

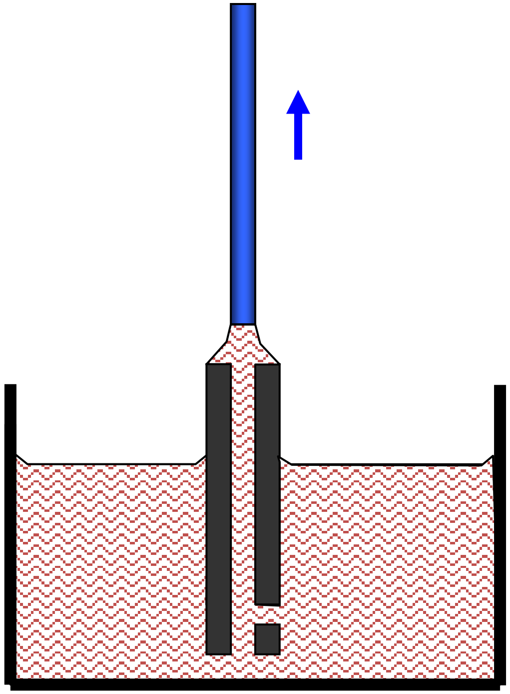

Edge-defined film-fed growth (EFG),

on the basis of the **Stepanov concept**

cross-sections of shaped crystals are very close to the final geometry
minimizing volume of labor efforts and corresponding losses of materials
growth of crystals with shapes which impossible to grow or prepare from bulk crystals
high growth rates
new fields of applications

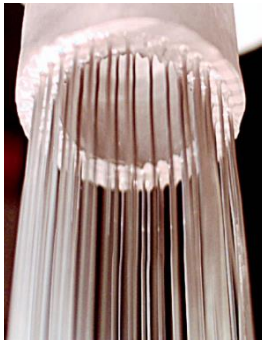

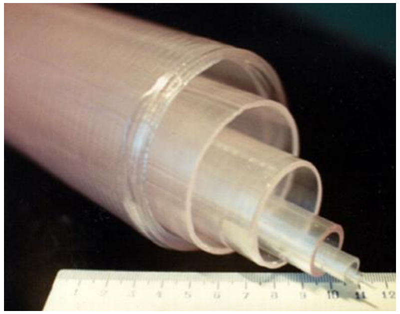

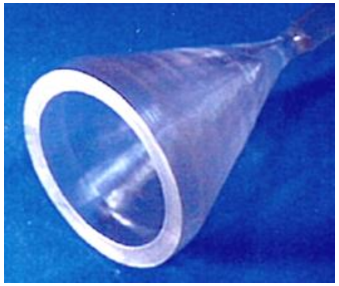

THz Waveguide Manufacturing Based on Shaped Sapphire Crystal

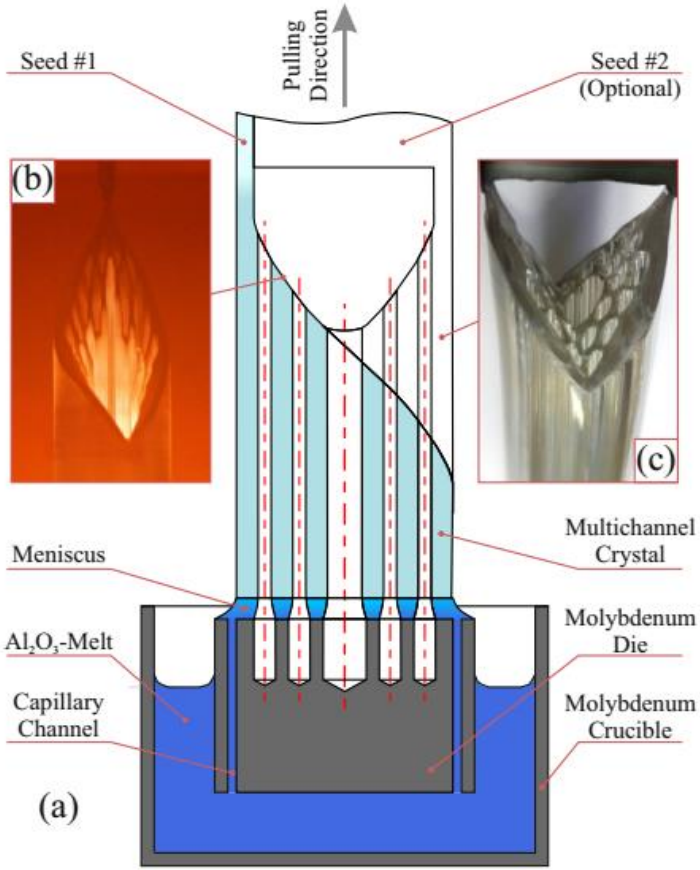

ARROW sapphire waveguide

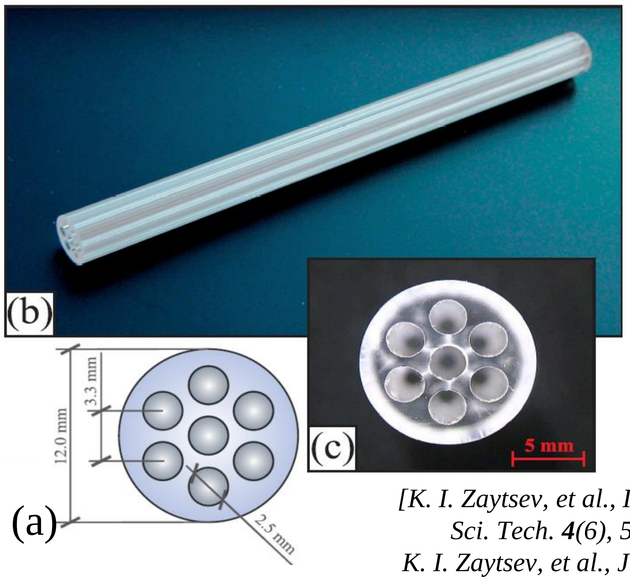

*[K. I. Zaytsev, et al., IEEE Trans. Ter. Sci. Tech. **4**(6), 576, (2016); K. I. Zaytsev, et al., J.Phys.Conf.Ser., **673**(1), 012001 (2016)].*

PC sapphire waveguide

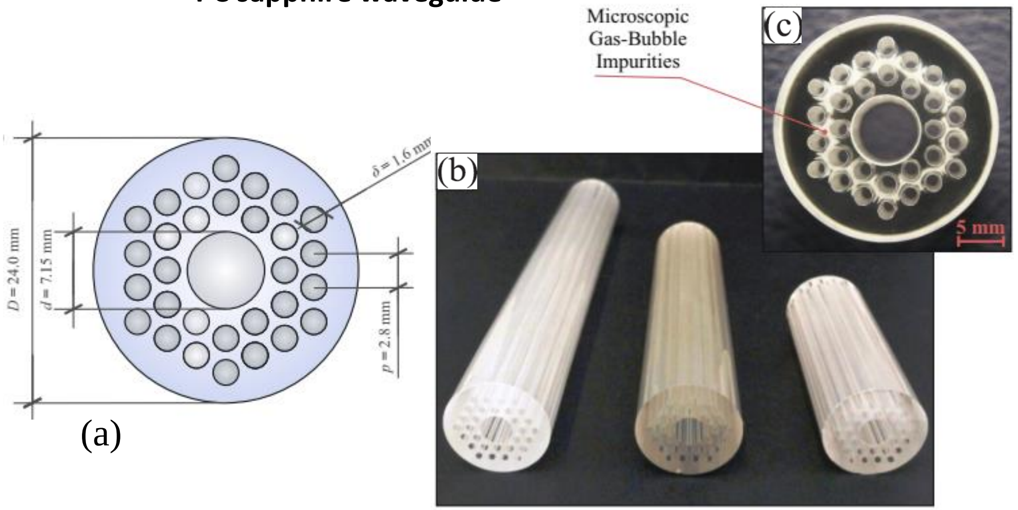

*[V. N. Kurlov and S. N. Rossolenko, J. Cryst. Growth **173**(3–4), 417–426 (1997); P. I. Antonov and V. N. Kurlov, Cryst. Reports **47**(1), S43–S52 (2002); G.M. Katyba, et.al., Proc.of SPIE, 103331C (2017); Katyba, G.M. et al., Progress in Crystal Growth and Characterization of Materials (2018)].*

THz Waveguiding in Shaped Sapphire: Numerical Analysis and Experimental Results

Dispersion curves for hollow-core waveguiding modes

THz time-domain spectrometer

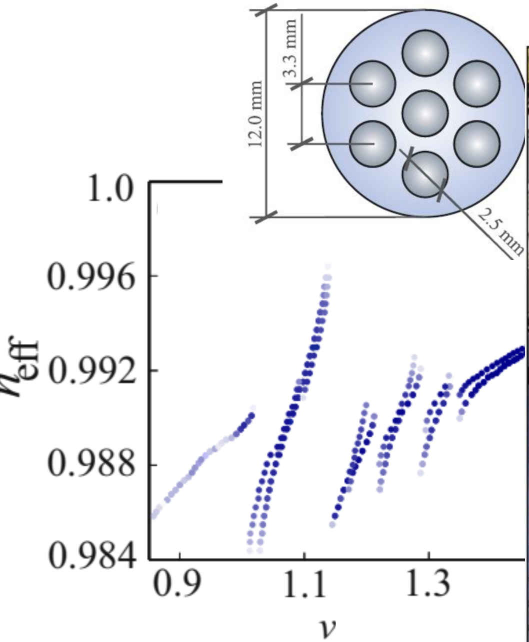

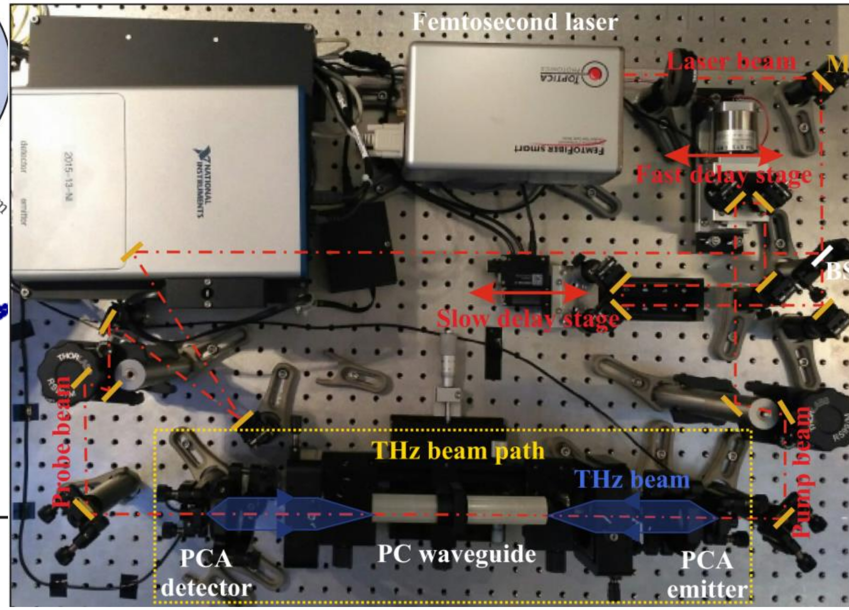

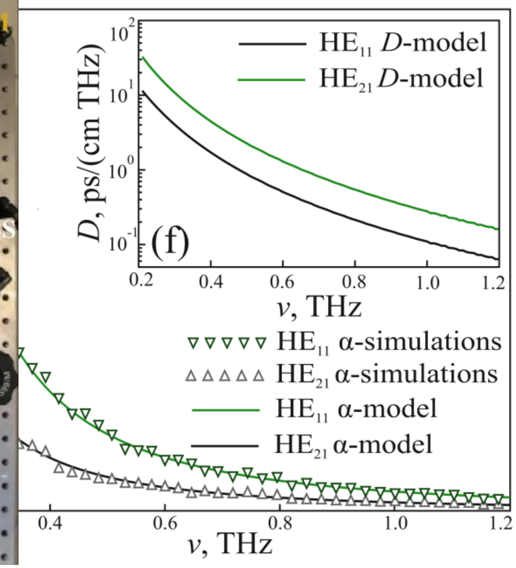

[G.M. Katyba, et al., Adv.Opt.Mat.,(2018); K. I. Zaytsev, et al., IEEE Trans. Ter. Sci. Tech. 4(6), 576, (2016)].

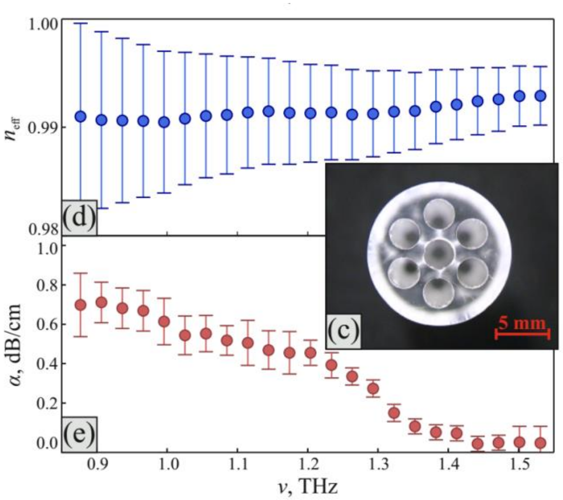

A model-based approximation of the experimental THz PC waveguide transmission

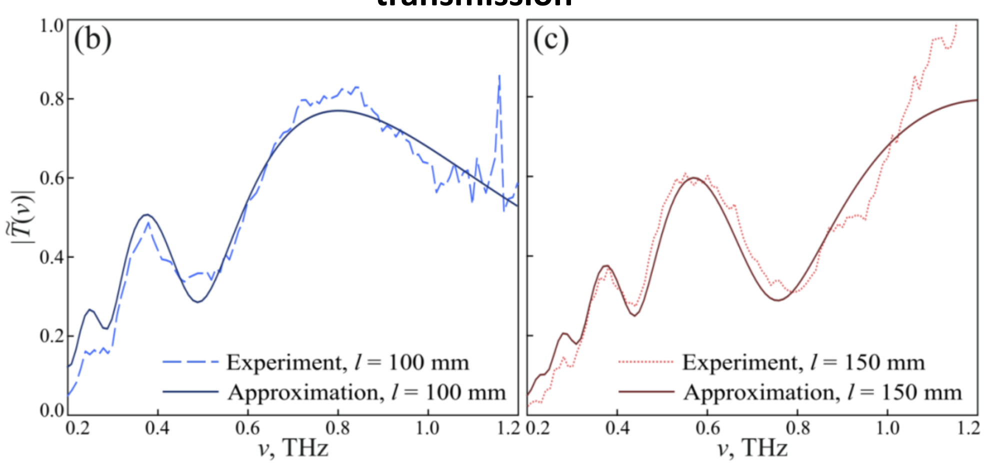

Attempts to improve the spatial resolution of THz imaging

INCREASING OF SPATIAL RESOLUTION OF THZ SENSING AND VISUALIZATION

Problem of low spatial resolution of THz spectroscopy and imaging

Standard focusing systems

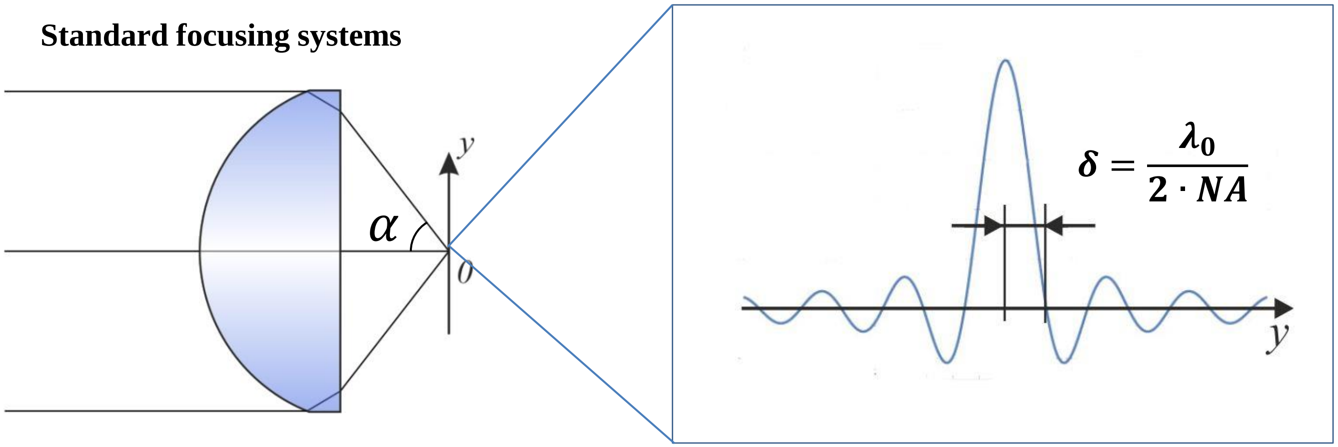

Spatial resolution (SP) is limited by electromagnetic wavelength ($\lambda \cong \mathbf{300}\ \mu m$ or 1 THz) and numerical aperture NA = $\boldsymbol{n \cdot sin\alpha}$

$$\boldsymbol{max\{NA\} = n}$$

$$\boldsymbol{\delta = \frac{\lambda_0}{2 \cdot n}}$$

Abbe diffraction limit

For n=1 (air) $\boldsymbol{\delta = \frac{\lambda_0}{2}}$

It is necessary to increase the NA to achieve high SP

$\uparrow NA \Rightarrow$ raise of aberrations

THZ IMAGING USING THE FIBER BUNDLES

Example: microwave fiber endoscope

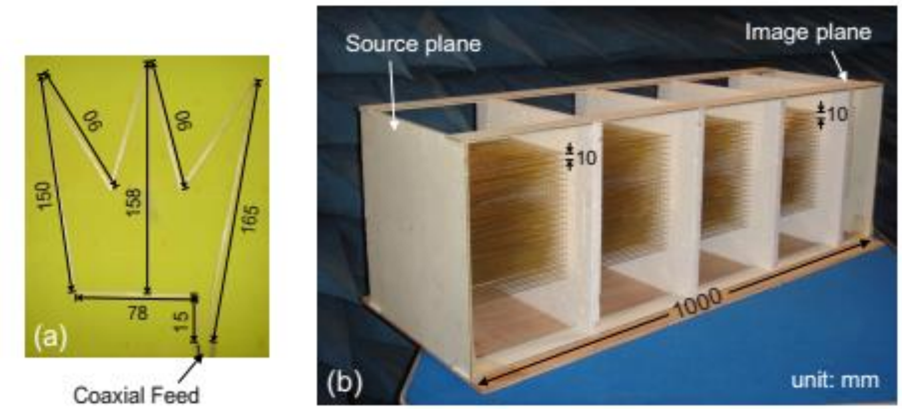

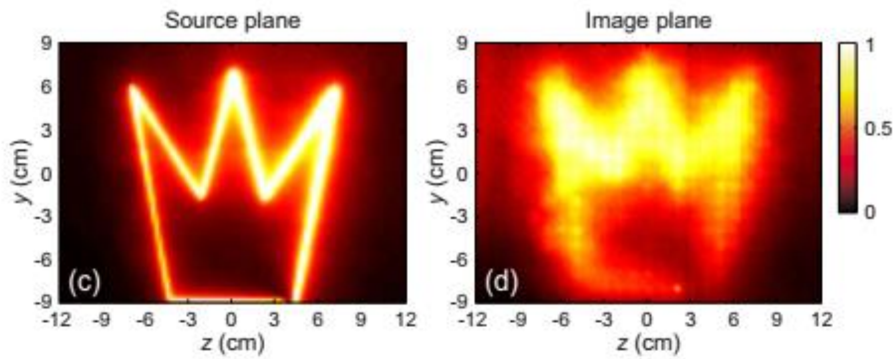

Minimal resolution– λ/200

[Belov P. A., et al. Appl. Phys. Lett. 97, 191905 (2010)]

$$\lambda_{m,n}^{\mathrm{TM}} = \frac{\pi n_{\mathrm{core}} d}{\gamma_{m,n}}, \qquad \lambda_{m,n}^{\mathrm{TE}} = \frac{\pi n_{\mathrm{core}} d}{\psi_{m,n}}$$

A concept of sapphire fiber bundle for THz imaging with sub-wavelength resolution

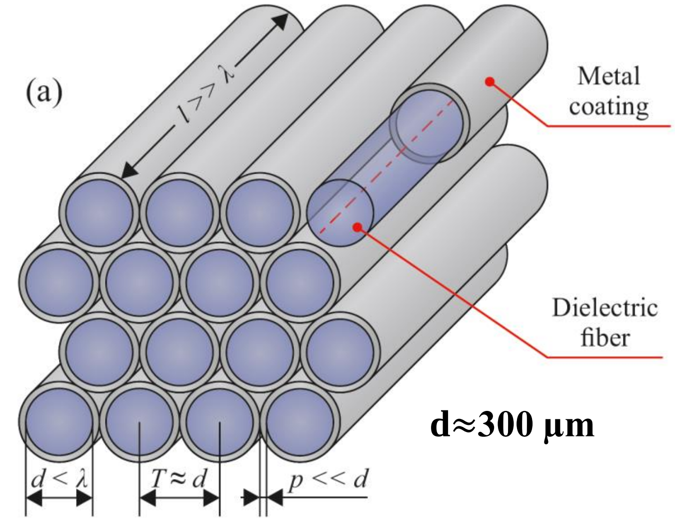

d≈300 µm

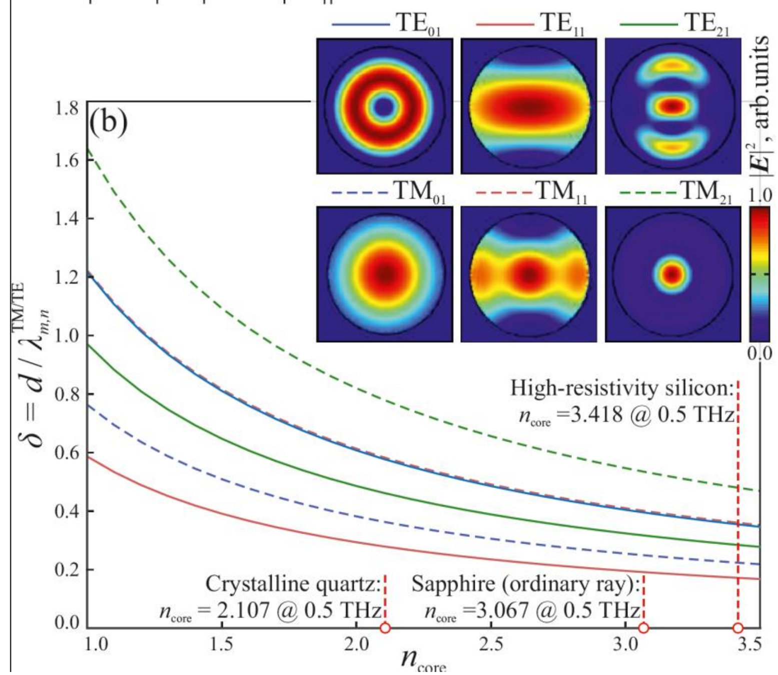

THZ IMAGING RELYING ON A BUNDLE OF METAL-COATED SAPPHIRE FIBERS:

Optical characterization

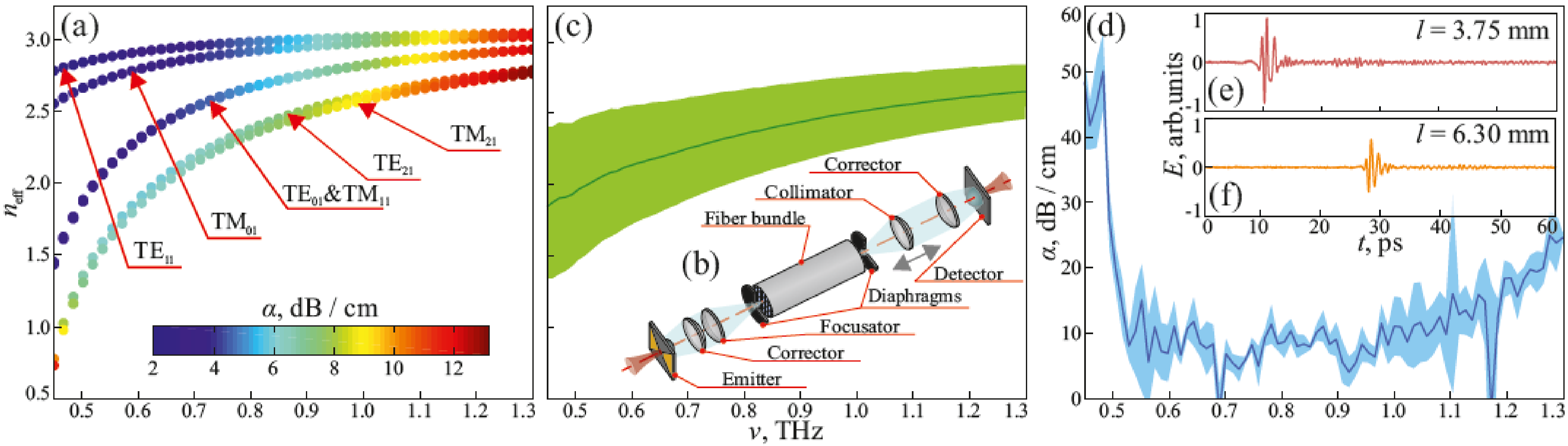

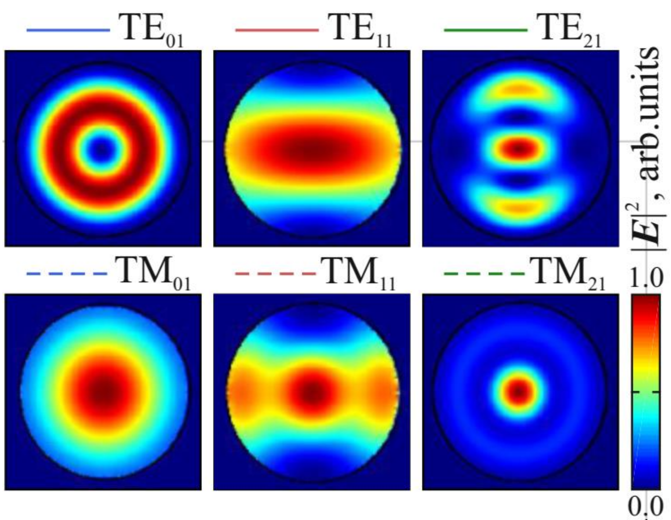

$$n_{\mathrm{eff}} = 1 + \frac{c_0}{2\pi\nu}\frac{1}{(l_2 - l_1)}\phi\left[\frac{\mathrm{F}_t^{+1}[E_2]}{\mathrm{F}_t^{+1}[E_1]}\right],$$

$$\alpha = \frac{-20}{(l_2 - l_1)}\lg\left|\frac{\mathrm{F}_t^{+1}[E_2]}{\mathrm{F}_t^{+1}[E_1]}\right|,$$

[K.I. Zaytsev et al., *Advanced Optical Materials* (2020), 2020, 2000307]

THZ IMAGING RELYING ON A BUNDLE OF METAL-COATED SAPPHIRE FIBERS

Sample of sapphire bundle

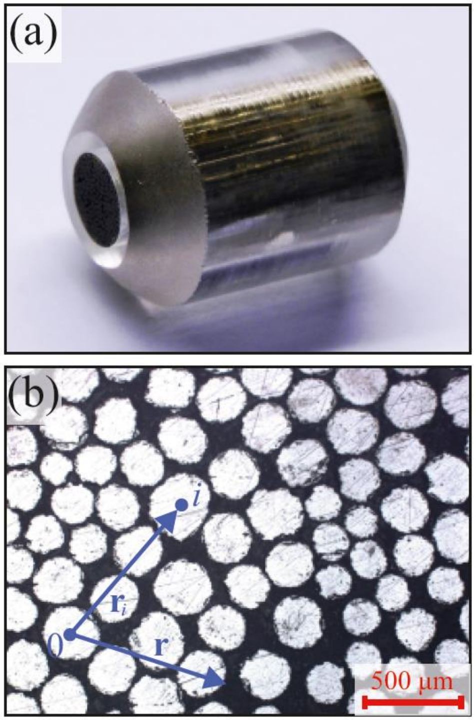

Resolution characterization $\langle \boldsymbol{\delta} \rangle = 0.53\,\lambda$

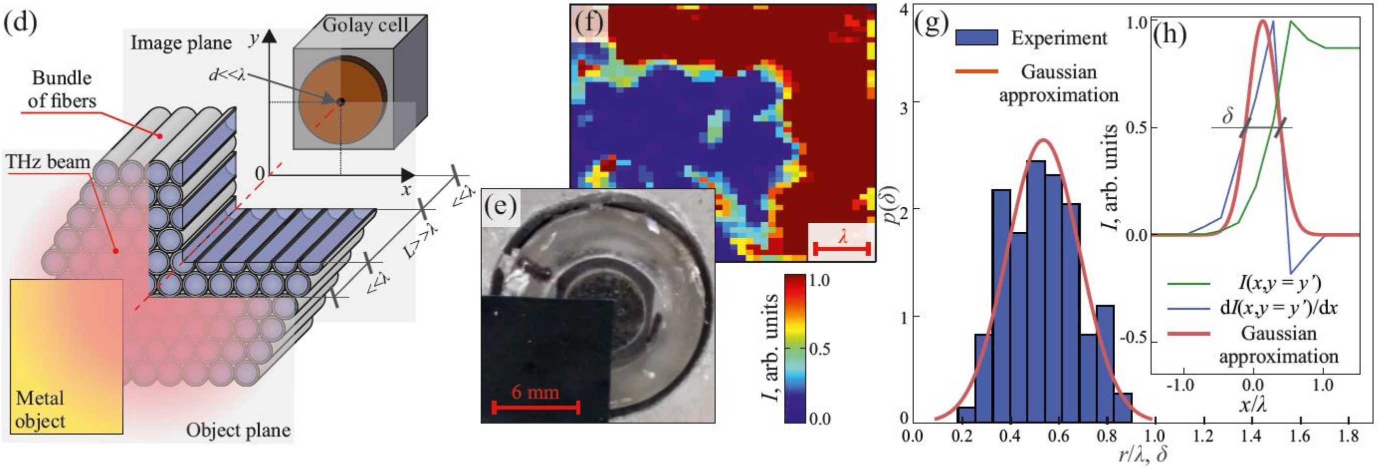

THz imaging of the test object

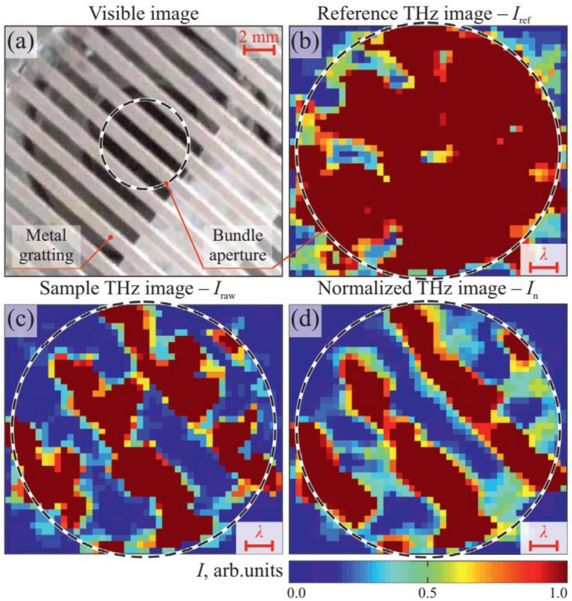

$$I_n(\mathbf{r}) = \frac{I_{raw}(\mathbf{r})}{I_{ref}(\mathbf{r})}\left(1 + \kappa \frac{N}{I_{ref}(\mathbf{r})}\right)^{-1}$$

DISADVANTAGES:
energy-inefficient near-field probes (apertures)

TAPERED ALL-DIELECTRIC OPTICAL BUNDLES FOR SUB WAVELENGTH IMAGING WITH USING DIFFRACTION LIMITED OPTICS

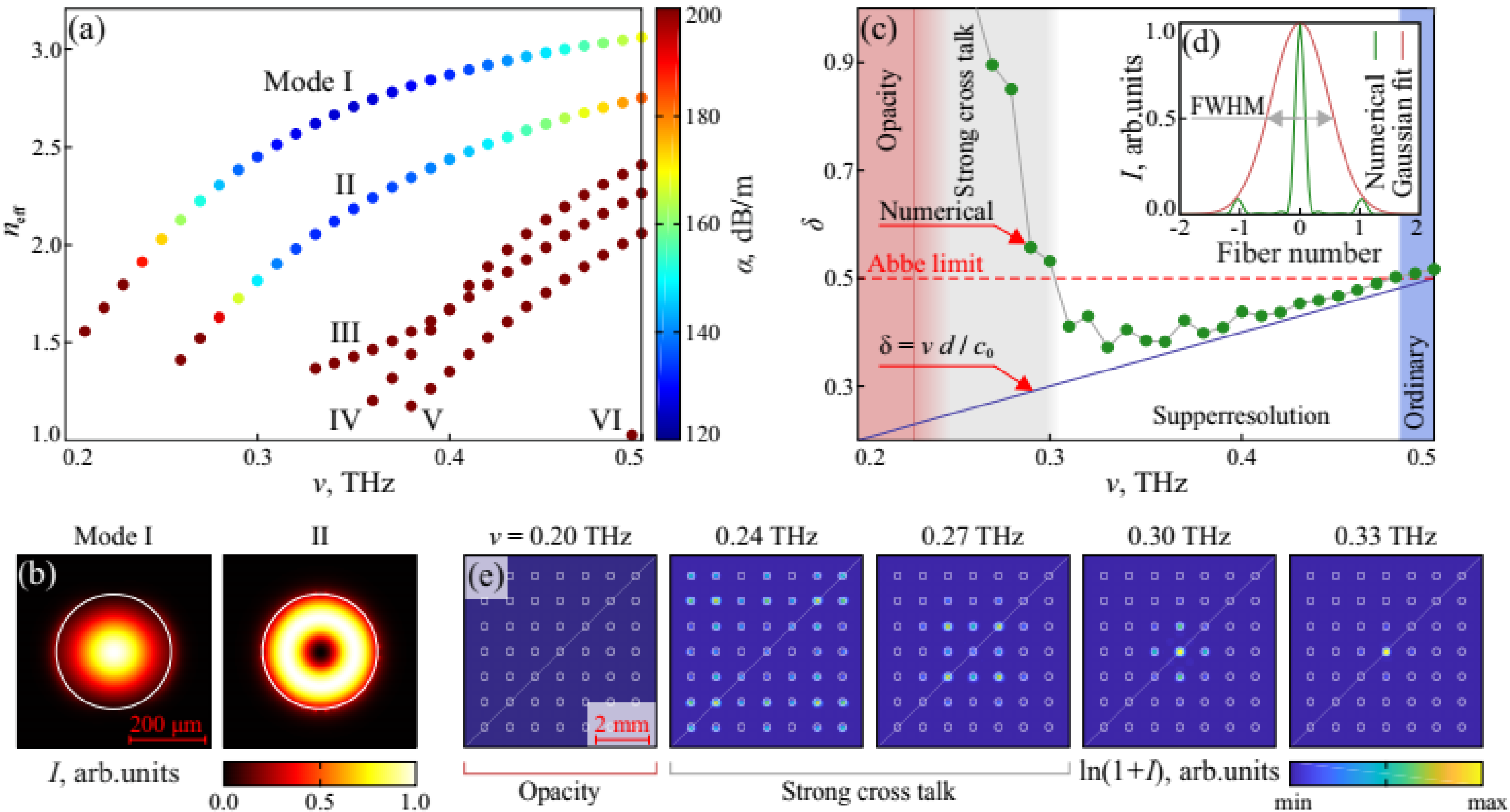

TAPERED ALL-DIELECTRIC OPTICAL BUNDLES FOR SUB WAVELENGTH IMAGING WITH USING DIFFRACTION LIMITED OPTICS

A concept of tapered sapphire fiber bundle for THz imaging with sub-wavelength resolution

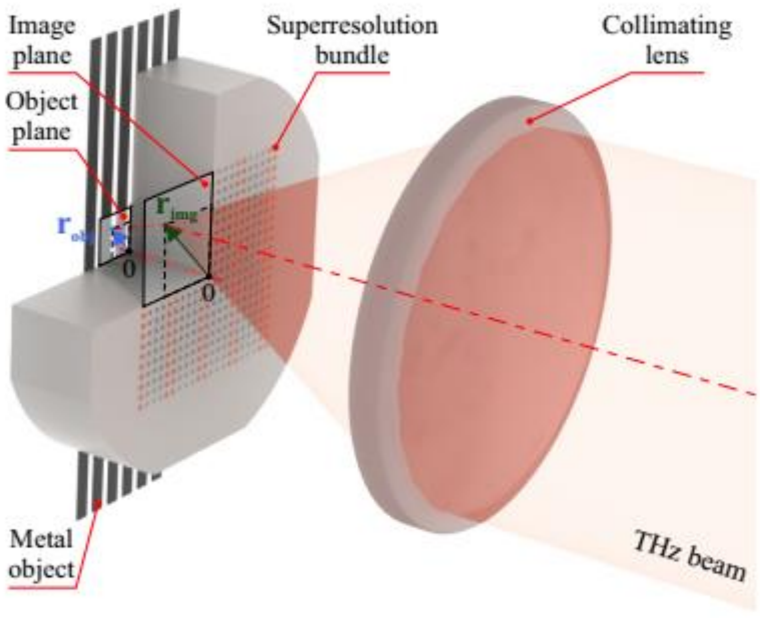

$$\delta = \frac{d}{\lambda} = \frac{d\nu}{c_0}.$$

Manufacturing of the sapphire fiber bundle for THz imaging with sub-wavelength resolution

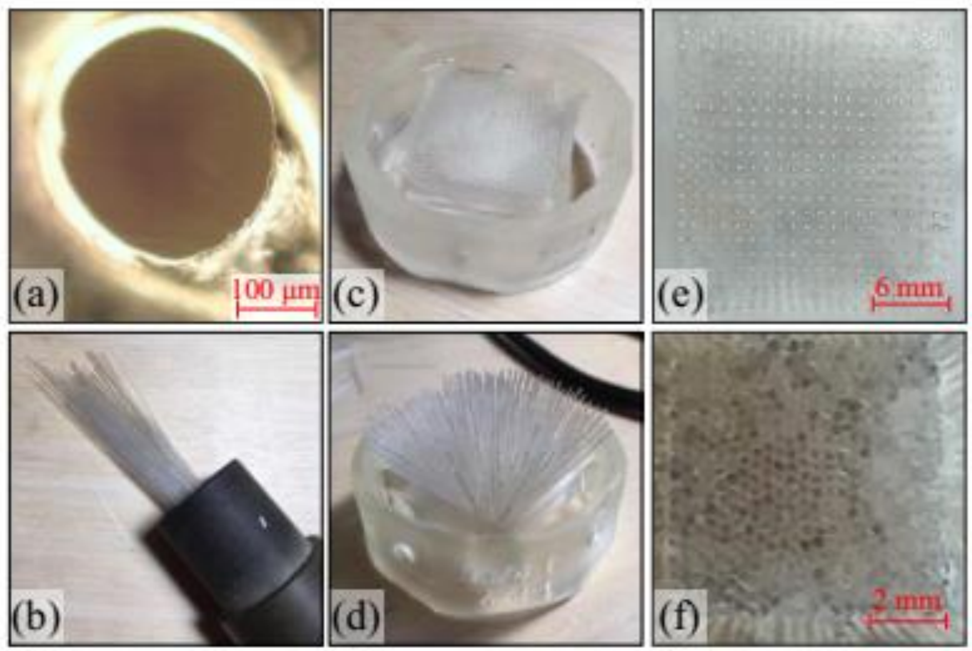

TAPERED ALL-DIELECTRIC OPTICAL BUNDLES FOR SUB WAVELENGTH IMAGING WITH USING DIFFRACTION LIMITED OPTICS

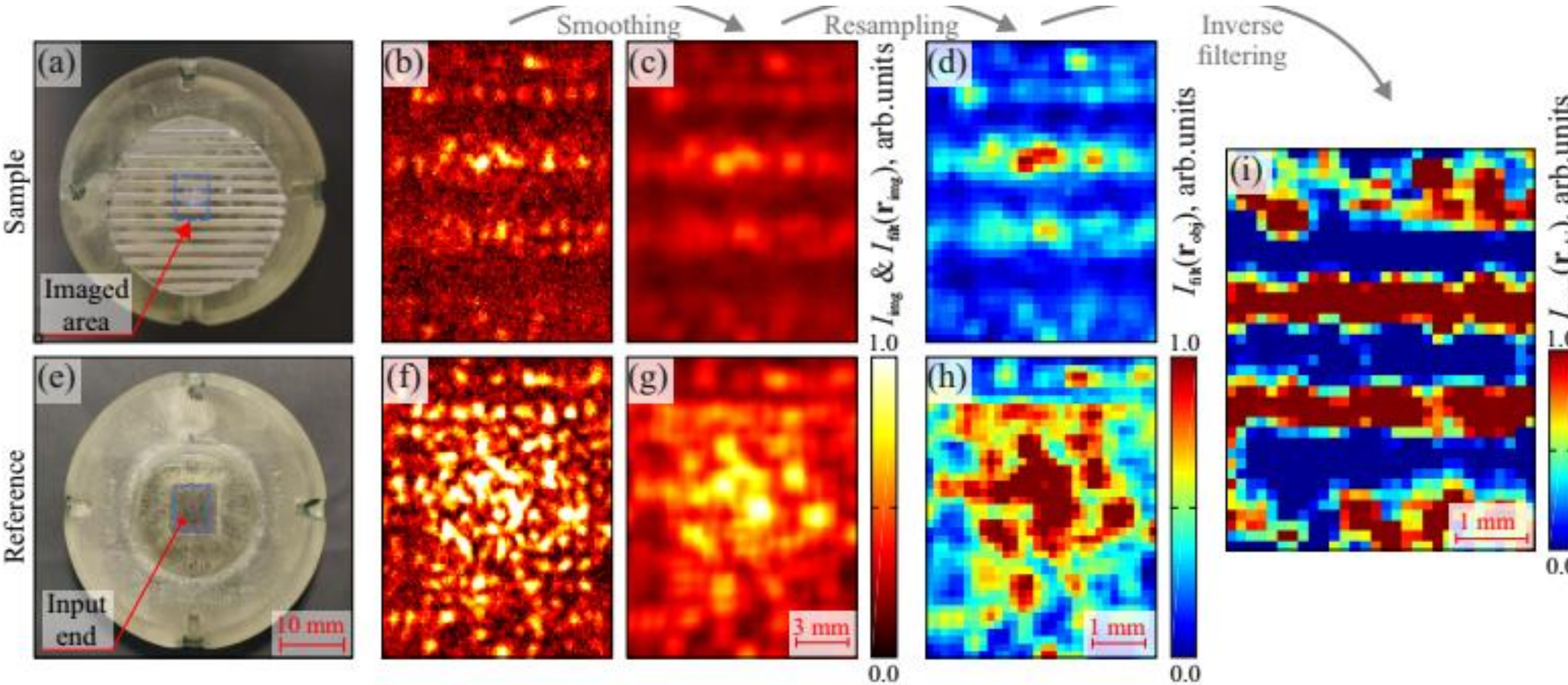

TAPERED ALL-DIELECTRIC OPTICAL BUNDLES FOR SUB WAVELENGTH IMAGING WITH USING DIFFRACTION LIMITED OPTICS

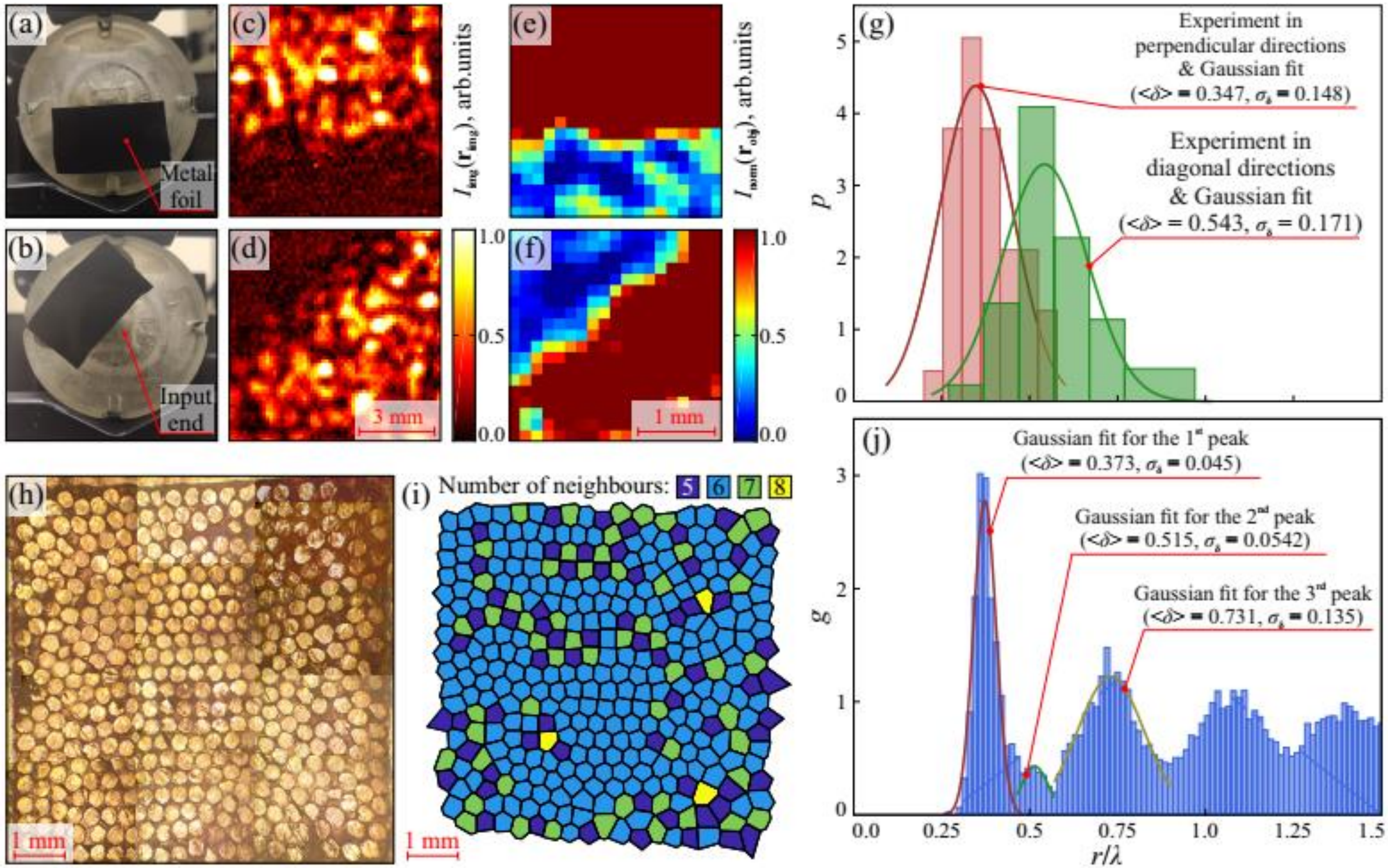

$$\langle \boldsymbol{\delta} \rangle \approx 0.34\,\lambda$$

RESEARCH GROUP & COLLABORATIONS

ISSP RAS
Chernogolovka, Russia


V.N. Kurlov


G.M. Katyba


V.E. Ulitko


A.S. Kucheryavenko


I.N. Dolganova


A.K. Zotov

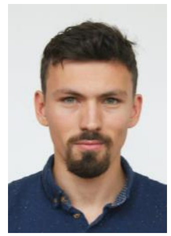
A.V. Kaledin

BMSTU
Moscow, Russia


D. E. Melikyants


E. V. Yakovlev

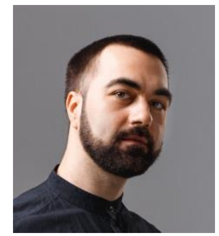
A. N. Perov

Sechenov University,
Moscow, Russia


I.V. Reshetov

Saratov State University,
Saratov, Russia


V.V. Tuchin

GPI RAS
Moscow, Russia


K.I. Zaytsev


G.A. Komandin


I.E. Spector


N.V. Chernomyrdin


A.A. Gavdush


V.A. Zhelnov


G.R. Musina

ILP SB RAS
Novosibirsk, Russia


O. P. Cherkasova

ITMO UNIVERSITY

ITMO University,
Saint-Petersburg, Russia


O.A. Smolyanskaya

ИСВЧПЭ РАН

IUHFSE RAS
Moscow, Russia


D.S. Ponomarev

Polytechnique Montreal
Montreal, Canada


M. Skorobogatiy

THANK YOU FOR ATTENTION!